SONOCHEMISTRY

Ultrasonic irradiation of liquids causes high energy chemical reactions to occur, often with the emission of light (1–5). The origin of sonochemistry and sonoluminescence is acoustic cavitation: the formation, growth, and implosive collapse of bubbles in liquids irradiated with high intensity sound. The collapse of bubbles caused by cavitation produces intense local heating and high pressures, with very short lifetimes. In clouds of cavitating bubbles, these hot-spots (6,7) have equivalent temperatures of roughly 5000 K, pressures of about 1000 atmospheres, and

Reprinted from
Kirk-Othmer *Encyclopedia of Chemical Technology, Fourth Edition, Supplement*
ISBN 0-471-52696-7

heating and cooling rates above 10^{10} K/s. In single-bubble cavitation, conditions may be even more extreme. Thus, cavitation can create extraordinary physical and chemical conditions in otherwise cold liquids.

When liquids that contains solids are irradiated with ultrasound, related phenomena can occur. When cavitation occurs near an extended solid surface, cavity collapse is nonspherical and drives high-speed jets of liquid into the surface (8,9). These jets and associated shock waves can cause substantial surface damage and expose fresh, highly heated surfaces. Ultrasonic irradiation of liquid–powder suspensions produces another effect: high velocity interparticle collisions. Cavitation and the shockwaves it creates in a slurry can accelerate solid particles to high velocities (10). The resultant collisions are capable of inducing dramatic changes in surface morphology, composition, and reactivity (11).

Sonochemistry can be roughly divided into categories based on the nature of the cavitation event: homogeneous sonochemistry of liquids, heterogeneous sonochemistry of liquid–liquid or liquid–solid systems, and sonocatalysis (which overlaps the first two) (12–15). In some cases, ultrasonic irradiation can increase reactivity by nearly a million-fold (16). Because cavitation can only occur in liquids, chemical reactions are not generally seen in the ultrasonic irradiation of solids or solid-gas systems.

Sonoluminescence in general may be considered a special case of homogeneous sonochemistry; however, recent discoveries in this field have heightened interest in the phenomenon in and by itself (17,18). Under conditions where an isolated, single bubble undergoes cavitation, recent studies on the duration of the sonoluminescence flash suggest that a shock wave may be created within the collapsing bubble, with the capacity to generate truly enormous temperatures and pressures within the gas.

Acoustic Cavitation

The chemical effects of ultrasound do not arise from a direct interaction with molecular species. Ultrasound spans the frequencies of roughly 15 kHz to 1 GHz. With sound velocities in liquids typically about 1500 m/s, acoustic wavelengths range from roughly 10 to 10^{-4} cm. These are not molecular dimensions. Consequently, no direct coupling of the acoustic field with chemical species on a molecular level can account for sonochemistry or sonoluminescence.

Instead, sonochemistry and sonoluminescence derive principally from acoustic cavitation (9), which serves as an effective means of concentrating the diffuse energy of sound. Compression of a gas generates heat. The compression of bubbles during cavitation is more rapid than thermal transport, which generates a short-lived, localized hot-spot. There is a general consensus that this hot-spot is the source of homogeneous sonochemistry. Rayleigh's early description of a mathematical model for the collapse of cavities in incompressible liquids predicted enormous local temperatures and pressures (19). Ten years later, Richards and Loomis reported the first chemical and biological effects of ultrasound (20). Alternative mechanisms involving electrical microdischarge have been occasionally proposed (21,22), but remain a minority viewpoint.

If the acoustic pressure amplitude of a propagating acoustic wave is relatively large (greater than ≈0.5 MPa), local inhomogeneities in the liquid (eg, gas-filled crevices in particulates) can give rise to the explosive growth of a nucleation site into a cavity of macroscopic dimensions, primarily filled with vapor. Such a bubble is inherently unstable, and its subsequent collapse can result in an enormous concentration of energy (Fig. 1). This violent cavitation event has been termed "transient cavitation" (23). A normal consequence of this unstable growth and subsequent collapse is that the cavitation bubble itself is destroyed. Gas-filled remnants from the collapse, however, may give rise to reinitiation of the process.

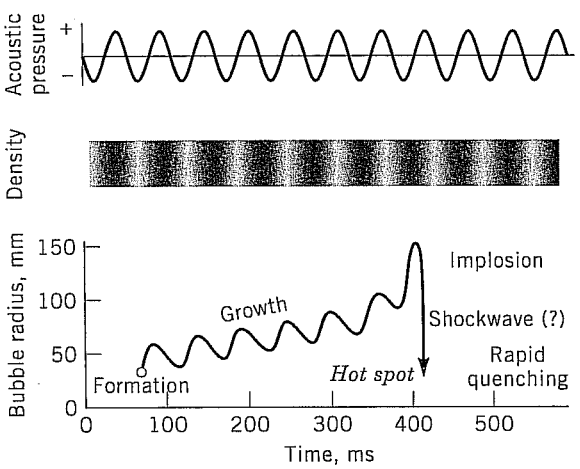

Fig. 1. Transient acoustic cavitation: the origin of sonochemistry and sonoluminescence.

The generally accepted explanation for the origin of sonochemistry and sonoluminescence is the hot-spot theory, in which the potential energy given the bubble as it expands to maximum size is concentrated into a heated gas core as the bubble implodes. The oscillations of a gas bubble driven by an acoustic field are generally described by Rayleigh-Plesset equation; one form of which, called the Gilmore equation (9,23), can be expressed a second-order nonlinear differential equation given as

$$R\left(1-\frac{U}{C}\right)\frac{d^2R}{dt^2}+\frac{3}{2}\left(1-\frac{U}{3C}\right)\left(\frac{dR}{dt}\right)^2-\left(1+\frac{U}{C}\right)H-\frac{R}{C}\left(1-\frac{U}{C}\right)\frac{dH}{dt}=0 \tag{1}$$

The radius and velocity of the bubble wall are given by R and U respectively. The values for H, the enthalpy at the bubble wall, and C, the local sound speed, may be expressed as follows, using the Tait equation of state for the liquid.

$$H=\frac{n}{n-1}\frac{A^{1/n}}{\rho_o}\left[(P(R)+B)^{n-1/n}-(P_\infty(t)+B)^{n-1/n}\right] \tag{2}$$

and

$$C = [c_o^2 + (n - 1)H] \tag{3}$$

The linear speed of sound in the liquid is c_o. A, B, and n are constants that should be set to the appropriate values for water. Any acoustic forcing function is included in the pressure at infinity term, $P_\infty(t)$. The pressure at the bubble wall, $P(R)$, is given by

$$P(R) = \left(P_o + \frac{2\sigma}{R}\right)\left(\frac{R_o}{R}\right)^{3\gamma} - \frac{2\sigma}{R} - \frac{4\mu U}{R} \tag{4}$$

where the initial radius of the bubble at time zero is R_o. The ambient pressure of the liquid is P_o, the surface tension σ, the shear viscosity μ, and the polytropic exponent γ.

The validity of the Gilmore equation to compute the behavior of a single, isolated cavitating bubble has been experimentally confirmed. For example, using a light scattering technique, various researchers have obtained measurements of the radius-time curve for single collapsing bubbles, simultaneous with optical emission from sonoluminescence (see below). The single-bubble sonoluminescent emission is seen as a sharp spike, appearing at the final stages of bubble collapse, and the general shape of the theoretical radius-time curve is observed (24–26).

Two-Site Model of Sonochemical Reactivity

The transient nature of the cavitation event precludes conventional measurement of the conditions generated during bubble collapse. Chemical reactions themselves, however, can be used to probe reaction conditions. The effective temperature realized by the collapse of clouds of cavitating bubbles can be determined by the use of competing unimolecular reactions whose rate dependencies on temperature have already been measured. This technique of comparative-rate chemical thermometry was used by Suslick, Hammerton, and Cline to first determine the effective temperature reached during cavity collapse (6). The sonochemical ligand substitutions of volatile metal carbonyls were used as these comparative rate probes (eq. 5, where the symbol $\xrightarrow{)))}$ represents ultrasonic irradiation of a solution, and L represents a substituting ligand). These kinetic studies revealed that there were in fact

$$\mathrm{M(CO)_x} \xrightarrow{)))} \mathrm{M(CO)_{x-n}} + n\ \mathrm{CO} \xrightarrow{\mathrm{L}} \mathrm{M(CO)_{x-n}(L)_n}$$

$$\text{where M} = \text{Fe, Cr, Mo, W} \tag{5}$$

two sonochemical reaction sites: the first (and dominant site) is the bubble's interior gas-phase while the second is an *initially* liquid phase. The latter corresponds either to heating of a shell of liquid around the collapsing bubble or to droplets of liquid ejected into the hot-spot by surface wave distortions of the collapsing bubble, as shown schematically in Figure 2.

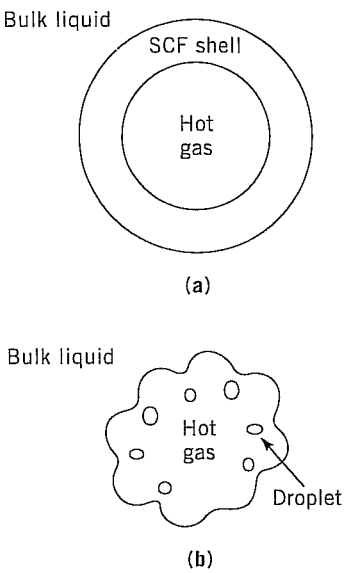

Fig. 2. Two-site models of the sonochemical reactions sites. (**a**) Thermal diffusion shell model; (**b**) surface wave droplet model.

The effective local temperatures in both sites were determined. By combining the relative sonochemical reaction rates for equation 5 with the known temperature behavior of these reactions, the conditions present during cavity collapse could then be calculated. The effective temperature of these hot-spots was measured at ≈5200 K in the gas-phase reaction zone and ≈1900 K in the initially liquid zone (6). Of course, the comparative rate data represent only a composite temperature: during the collapse, the temperature has a highly dynamic profile, as well as a spatial temperature gradient. This two-site model has been confirmed with other reactions (27,28) and alternative measurements of local temperatures by sonoluminescence are consistent (7), as discussed later.

Microjet Formation during Cavitation at Liquid–Solid Interfaces

A very different phenomenon arises when cavitation occurs near extended liquid–solid interfaces. There are two proposed mechanisms for the effects of cavitation near surfaces: microjet impact and shockwave damage. Whenever a cavitation bubble is produced near a boundary, the asymmetry of the liquid particle motion during cavity collapse can induce a strong deformation in the cavity (9). The potential energy of the expanded bubble is converted into kinetic energy of a liquid jet that extends through the bubble's interior and penetrates the opposite bubble wall. Because most of the available energy is transferred to the accelerating jet, rather than the bubble wall itself, this jet can reach velocities of hundreds of meters per second. Because of the induced asymmetry, the jet often impacts the solid boundary and can deposit enormous energy densities at

the site of impact. Such energy concentration can result in severe damage to the boundary surface. Figure 3 is a photograph of a jet developed in a collapsing cavity. The second mechanism of cavitation-induced surface damage invokes shockwaves created by cavity collapse in the liquid. The impingement of microjets and shockwaves on the surface creates the localized erosion responsible for much of ultrasonic cleaning and many of the sonochemical effects on heterogeneous reactions. In this process, the erosion of metals by cavitation generates newly exposed, highly heated surfaces that are highly reactive.

A solid surface several times larger than the resonance bubble size is necessary to induce distortions during bubble collapse. For ultrasound of ≈20 kHz, damage associated with jet formation cannot occur if the solid particles are smaller than ≈200 μm. In these cases, however, the shockwaves created by homogeneous cavitation can create high velocity interparticle collisions (10,11). Suslick and co-workers have found that the turbulent flow and shockwaves produced by intense ultrasound can drive metal particles together at sufficiently high speeds to induce effective melting in direct collisions (Fig. 4) and the abrasion of surface crystallites in glancing impacts (Fig. 5). A series of transition metal powders were used to probe the maximum temperatures and speeds reached during interparticle collisions. Using the irradiation of Cr, Mo, and W powders in decane at 20 kHz and 50 W/cm^2, agglomeration and essentially a localized melting occurs for the first two metals, but not the third (Fig. 6). On the basis of the melting points of these metals, the effective transient temperature reached at the point of impact during interparticle collisions is roughly 3000°C (which is unrelated to the temperature inside the hot-spot of a collapsing bubble). From the volume of the melted region of impact, the amount of energy generated during collision was determined. From this, a lower estimate of the velocity of impact is roughly one half the speed of sound (10). These are precisely the effects expected on suspended particulates from cavitation-induced shockwaves in the liquid.

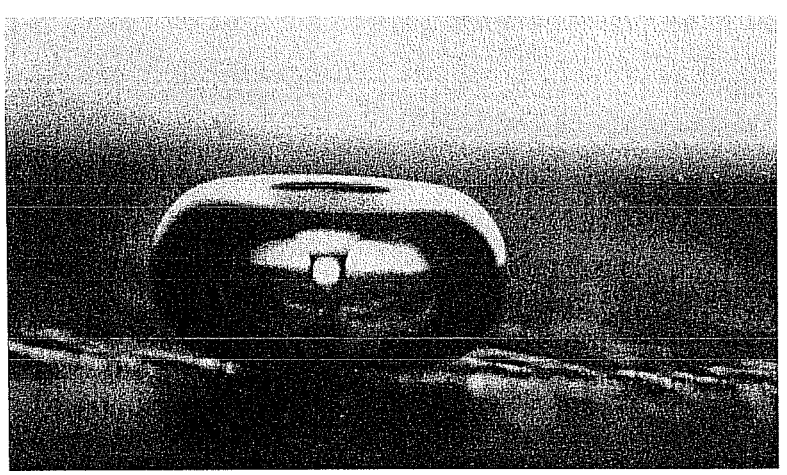

Fig. 3. Liquid jet produced during collapse of a cavitation bubble near a solid surface. The width of the bubble is about 1 mm. Reproduced with permission (8).

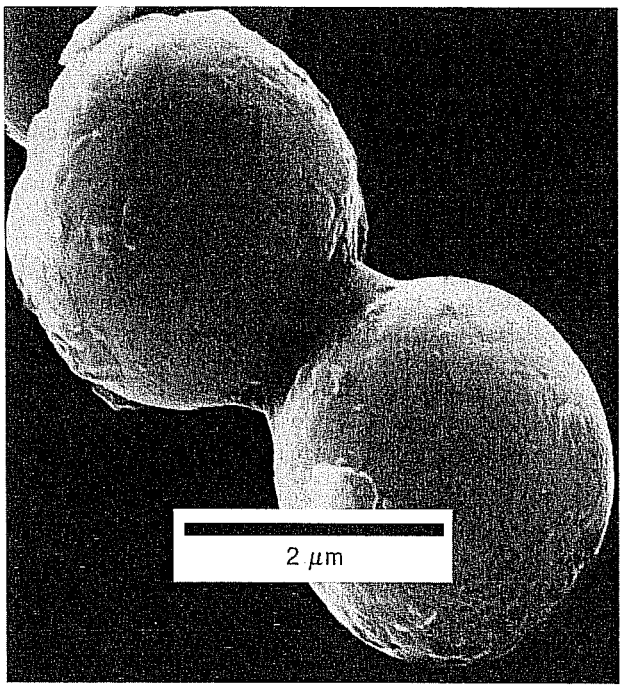

Fig. 4. Scanning electron micrograph of 5-μm diameter Zn powder. Neck formation from localized melting is caused by high-velocity interparticle collisions. Similar micrographs and elemental composition maps (by Auger electron spectroscopy) of mixed metal collisions have also been made. Reproduced with permission (10).

Sonoluminescence

Types of Sonoluminescence. In addition to driving chemical reactions, ultrasonic irradiation of liquids can also produce light. Sonoluminescence was first observed from water in 1934 by Frenzel and Schultes (29). As with sonochemistry, sonoluminescence derives from acoustic cavitation. It is now generally thought that there are two separate forms of sonoluminescence: multiple-bubble sonoluminescence (MBSL) and single-bubble sonoluminescence (SBSL) (17,24,30). Since cavitation is a nucleated process and liquids generally contain large numbers particulates that serve as nuclei, the cavitation field generated by propagating or standing acoustic wave typically consists of very large numbers of interacting bubbles, distributed over an extended region of the liquid. If this cavitation is sufficiently intense to produce sonoluminescence, then this phenomenon is called multiple-bubble sonoluminescence (MBSL) (2,17).

Under the appropriate conditions, the acoustic force on a bubble can be used to balance against its buoyancy, holding the single bubble isolated in the liquid by acoustic levitation. This permits examination of the dynamic characteristics of the bubble can in considerable detail, from both a theoretical and an experimental perspective. Such a bubble is typically quite small, compared to an acoustic wavelength (eg, at 20 kHz, the resonance size is approximately 150 μm). It was

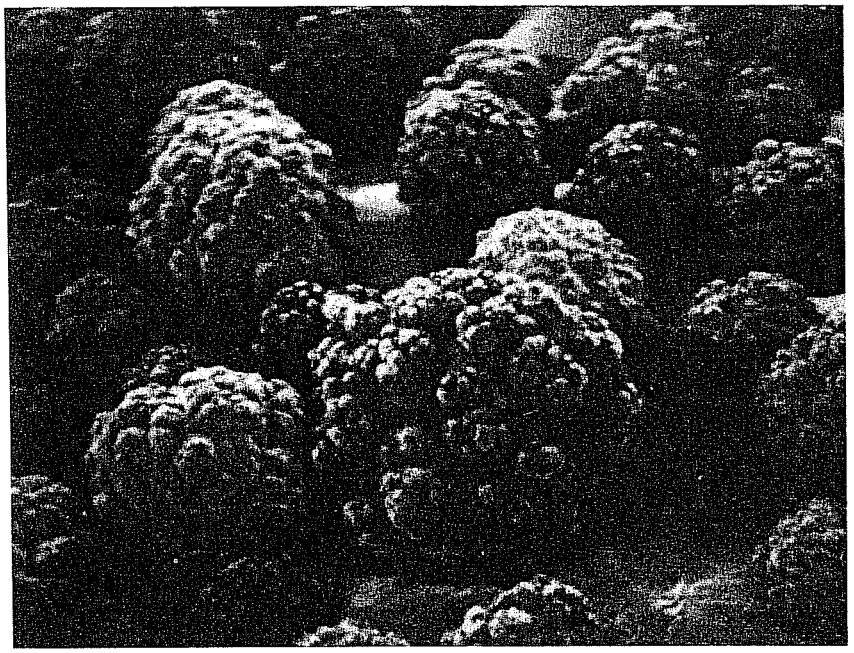

(a)

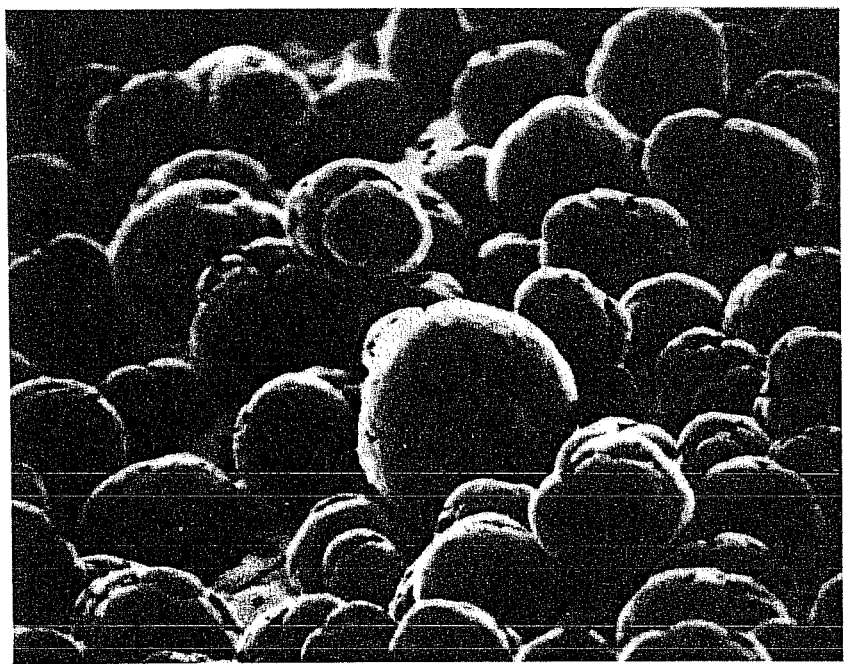

(b)

Fig. 5. The effect of ultrasonic irradiation on the surface morphology and particle size of Ni powder. Initial particle diameters (**a**) before ultrasound were ≈160 μm; (**b**) after ultrasound, ≈80 μm. High velocity interparticle collisions caused by ultrasonic irradiation of slurries are responsible for the smoothing and removal of passivating oxide coating. Reproduced with permission (11).

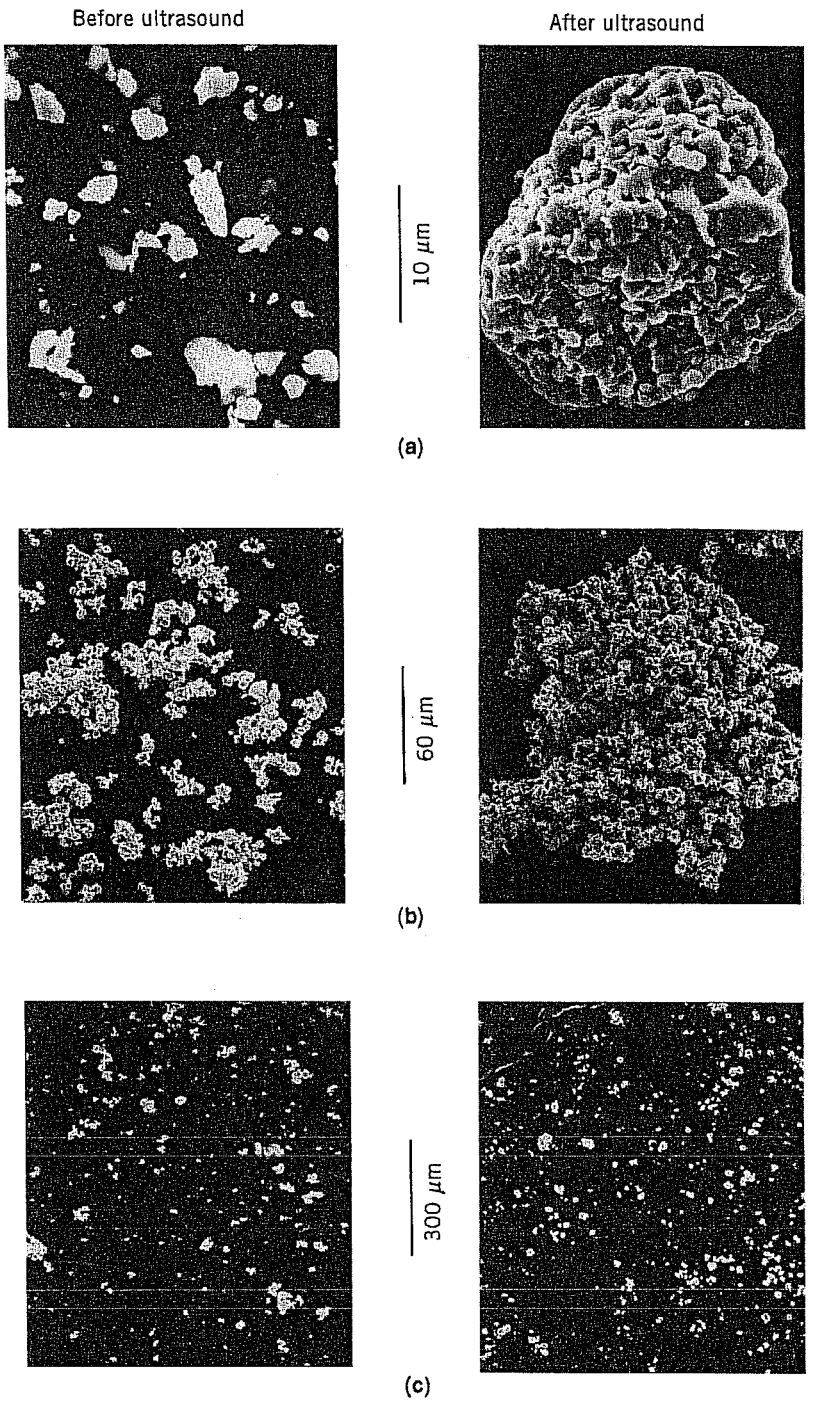

Fig. 6. The effect of ultrasound on particle agglomeration of (**a**) Cr (mp 1857°C), (**b**) Mo (mp 2617°C), and (**c**) W (mp 3410°C) after irradiation of decane slurries under Ar. Reproduced with permission (10).

recently discovered for rather specialized but easily obtainable conditions, that a single, stable, oscillating gas bubble can be forced into such large amplitude pulsations that it produces sonoluminescence emissions on each (and every) acoustic cycle (31,32). This phenomenon is called single-bubble sonoluminescence, and has received considerable recent attention (17,18,33,34).

Multiple-Bubble Sonoluminescence. The sonoluminescence of aqueous solutions has been often examined over the past thirty years. The spectrum of MBSL in water consists of a peak at 310 nm and a broad continuum throughout the visible region. An intensive study of aqueous MBSL was conducted by Verrall and Sehgal (35). The emission at 310 nm is from excited-state OH^*, but the continuum is difficult to interpret. MBSL from aqueous and alcohol solutions of many metal salts have been reported and are characterized by emission from metal atom excited states (36).

Sonoluminescence from nonaqueous liquids has only recently been examined. Flint and Suslick reported the first MBSL spectra of organic liquids (37). With various hydrocarbons, the observed emission is from excited states of C_2 ($d^3\Pi_g - a^3\Pi_u$, the Swan lines), the same emission seen in flames. Furthermore, the ultrasonic irradiation of alkanes in the presence of N_2 (or NH_3 or amines) gives emission from CN excited states, but not from N_2 excited states. Emission from N_2 excited states would have been expected if the MBSL originated from microdischarge, whereas CN emission is typically observed from thermal sources. When oxygen is present, emission from excited states of CO_2, CH·, and OH· is observed, again similar to flame emission.

For both aqueous and nonaqueous liquids, MBSL is caused by chemical reactions of high-energy species formed during cavitation by bubble collapse, and its principal source is most probably not blackbody radiation or electrical discharge. MBSL is predominantly a form of chemiluminescence.

Single-Bubble Sonoluminescence. The spectra of MBSL and SBSL are dramatically different. MBSL is generally dominated by atomic and molecular emission lines, but SBSL is an essentially featureless emission that increases with decreasing wavelength. For example, an aqueous solution of NaCl shows evidence of excited states of both OH· and Na in the MBSL spectrum; however, the SBSL spectrum of an identical solution shows no evidence of either of these peaks (30). Similarly, the MBSL spectrum falls off at low wavelengths, while the SBSL spectrum continues to rise, at least for bubbles containing most noble gases (38).

An intriguing aspect of SBSL is the extremely short duration of the sonoluminescence flash. The hydrodynamic models of adiabatic collapse of a single bubble suggest that the temperature of the gas within the bubble should remain at elevated temperatures for times on the order of tens of nanoseconds; however, there is strong evidence that the pulse duration of the SBSL flash is three orders of magnitude shorter. Putterman and his colleagues, using the fastest PMT available, reported that this duration is less than 50 ps, perhaps much less (39). The most plausible explanation for this short flash interval, and some of the observed spectra (see below), is that an imploding shock wave is created within the gas bubble during the final stages of collapse. If this shock wave does indeed exist, exciting possibilities can be inferred about the temperatures that could be attained within the bubble and the physics that might result. Indeed,

speculations on the possibilities of inertial confinement (*hot*) fusion have been made (40,41).

Spectroscopic Probes of Cavitation Conditions. Determination of the temperatures reached in a cavitating bubble has remained a difficult experimental problem. As a spectroscopic probe of the cavitation event, MBSL provides a solution. High resolution MBSL spectra from silicone oil under Ar have been reported and analyzed (7). The observed emission comes from excited state C_2 and has been modeled with synthetic spectra as a function of rotational and vibrational temperatures, as shown in Figure 7. From comparison of synthetic to observed spectra, the effective cavitation temperature is 5050 ± 150 K. The excellence of the match between the observed MBSL and the synthetic spectra provides definitive proof that the sonoluminescence event is a thermal, chemiluminescence process. The agreement between this spectroscopic determination of the cavitation temperature and that made by comparative rate thermometry of sonochemical reactions is surprisingly close (6).

The interpretation of the spectroscopy of SBSL is much less clear. At this writing, SBSL has been observed primarily in aqueous fluids, and the spectra obtained are surprisingly featureless. Some very interesting effects are observed when the gas contents of the bubble are changed (39,42). Furthermore, the spectra show practically no evidence of OH emissions, and when He and Ar bubbles are considered, continue to increase in intensity even into the deep ultraviolet. These spectra are reminiscent of black body emission with temperatures *considerably* in excess of 5000 K and lend some support to the concept of an imploding shock wave (41). Several other alternative explanations for SBSL have been presented, and there exists considerable theoretical activity in this particular aspect of SBSL.

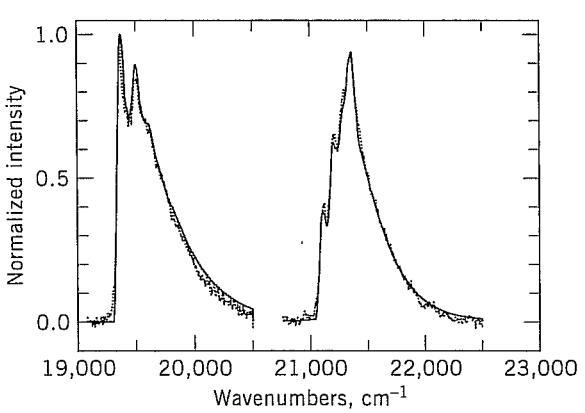

Fig. 7. Sonoluminescence of excited state C_2. Emission from the $\Delta v = +1$ manifold of the $d^3\Pi_g - a^3\Pi_u$ transition (Swan band) of C_2. Reproduced with permission (7). ·····, Observed sonoluminescence from polydimethylsiloxane silicone oil under Ar at 0°C; ———, best fit synthetic spectrum, with $T_v = T_r = 4900$ K.

Sonochemistry

In a fundamental sense, chemistry is the interaction of energy and matter. Chemical reactions require energy in one form or another to proceed: chemistry stops as the temperature approaches absolute zero. One has only limited control, however, over the nature of this interaction. In large part, the properties of a specific energy source determines the course of a chemical reaction. Ultrasonic irradiation differs from traditional energy sources (such as heat, light, or ionizing radiation) in duration, pressure, and energy per molecule. The immense local temperatures and pressures and the extraordinary heating and cooling rates generated by cavitation bubble collapse mean that ultrasound provides an unusual mechanism for generating high energy chemistry. Like photochemistry, very large amounts of energy are introduced in a short period of time, but it is thermal, not electronic, excitation. As in flash pyrolysis, high thermal temperatures are reached, but the duration is very much shorter (by $>10^4$) and the temperatures are even higher (by five- to ten-fold). Similar to shock-tube chemistry or multiphoton infrared laser photolysis, cavitation heating is very short lived, but occurs within condensed phases. Furthermore, sonochemistry has a high-pressure component, which suggests that one might be able to produce on a microscopic scale the same macroscopic conditions of high temperature–pressure "bomb" reactions or explosive shockwave synthesis in solids. Figure 8 presents an interesting comparison of the parameters that control chemical reactivity (time, pressure, and energy) for various forms of chemistry.

Experimental Design. A variety of devices have been used for ultrasonic irradiation of solutions. There are three general designs in use presently: the ultrasonic cleaning bath, the direct immersion ultrasonic horn, and flow reactors.

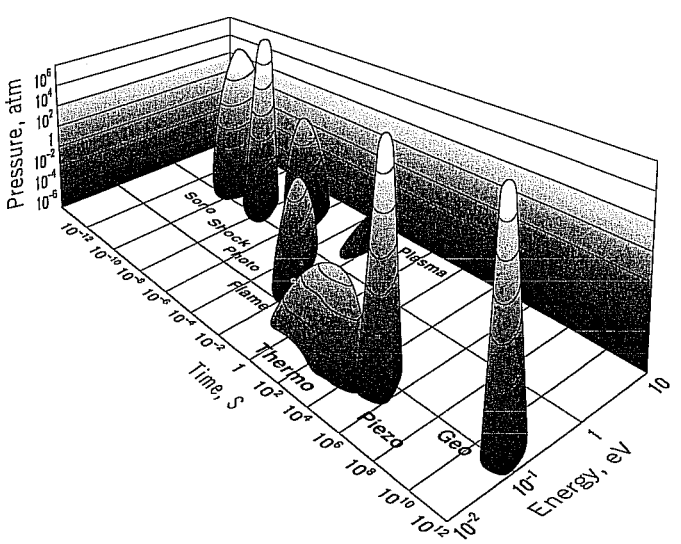

Fig. 8. Chemistry: the interaction of energy and matter. To convert atm to Pa, multiply by 1.013×10^5.

The originating source of the ultrasound is generally a piezoelectric material, usually a lead zirconate titanate ceramic (PZT), which is subjected to a high a-c voltage with an ultrasonic frequency (typically 15 to 50 kHz). For industrial use, the more robust magnetostrictive metal alloys (usually of Ni) can be used as the core of a solenoid generating an alternating magnetic field with an ultrasonic frequency. The vibrating source is attached to the wall of a cleaning bath, to an amplifying horn, or to the outer surfaces of a flow-through tube or diaphragm.

The ultrasonic cleaning bath is clearly the most accessible source of laboratory ultrasound and has been used successfully for a variety of liquid–solid heterogeneous sonochemical studies. Lower acoustic intensities can often be used in liquid–solid heterogeneous systems, because of the reduced liquid tensile strength at the liquid–solid interface. For such reactions, a common ultrasonic cleaning bath will therefore often suffice. The low intensity available in these devices ($\approx$1 W/cm^2), however, can prove limiting. In addition, the standing wave patterns in ultrasonic cleaners require accurate positioning of the reaction vessel. On the other hand, ultrasonic cleaning baths are easily accessible, relatively inexpensive, and usable on moderately large scale. Even in the case of heterogeneous sonochemistry, however, the ultrasonic cleaning bath must be viewed as an apparatus of limited capability.

The most intense and reliable source of ultrasound generally used in the chemical laboratory is the direct immersion ultrasonic horn (50 to 500 W/cm^2), as shown in Figure 9, which can be used for work under either inert or reactive atmospheres or at moderate pressures (<10 atmospheres). These devices are available from several manufacturers at modest cost and are often used by biochemists for cell disruption. A variety of sizes of power supplies and titanium horns are available, thus allowing flexibility in sample size. Commercially available flow-through reaction chambers which will attach to these horns allow the processing of multiliter volumes. The acoustic intensities are easily and reproducibly variable; the acoustic frequency is well controlled, albeit fixed (typically at 20 kHz). Since power levels are quite high, counter-cooling of the reaction solution is essential to provide temperature control. Erosion of the titanium tip is a potential disadvantage, especially in corrosive media. Such erosion is generally a very slow process without chemical consequences (given the high tensile strength and low reactivity of Ti metal) and can be avoided by using the horn to irradiate through a cooling solution into a reaction solution held in a glass container (a so-called cup-horn).

Large-scale ultrasonic generation in flow-through configurations is a well-established technology (43–46). Liquid processing rates as high as 200 L/min are routinely accessible from a variety of modular, in-line designs with acoustic power of $\approx$20 kW per unit. The industrial uses of these units include (*1*) degassing of liquids, (2) dispersion of solids into liquids, (*3*) emulsification of immiscible liquids and (*4*) large-scale cell disruption (45,46).

Homogeneous sonochemistry typically is not a very energy efficient process (although it can be more efficient than photochemistry), whereas heterogeneous sonochemistry is several orders of magnitude better. Unlike photochemistry, whose energy inefficiency is inherent in the production of photons, ultrasound

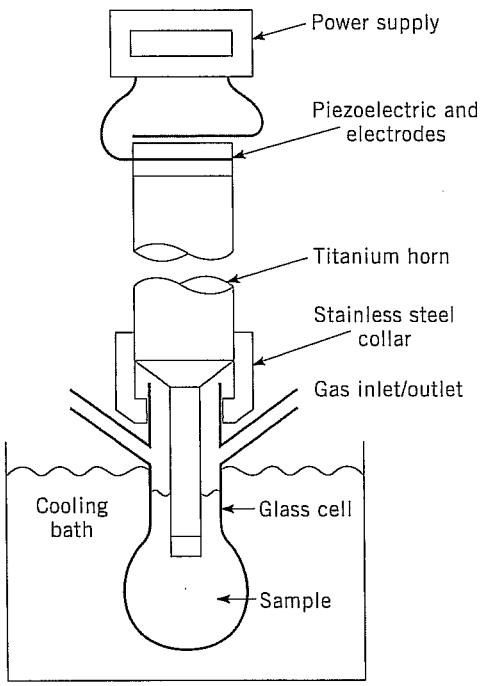

Fig. 9. A typical sonochemical apparatus with direct immersion ultrasonic horn. Ultrasound can be easily introduced into a chemical reaction with good control of temperature and ambient atmosphere. The usual piezoelectric ceramic is PZT, a lead zirconate titanate ceramic. Similar designs for sealed stainless steel cells can operate at pressures above 10 bar.

can be produced with nearly perfect efficiency from electric power. A primary limitation of sonochemistry remains the small fraction of the acoustic power actually involved in the cavitation events. This might be significantly improved, however, if a more efficient means of coupling the sound field to generate cavitation can be found.

Sonochemistry is strongly affected by a variety of external variables, including acoustic frequency, acoustic intensity, bulk temperature, static pressure, ambient gas, and solvent (47). These are the important parameters which need consideration in the effective application of ultrasound to chemical reactions. The origin of these influences is easily understood in terms of the hot-spot mechanism of sonochemistry.

The frequency of the sound field is not a commonly altered variable in most sonochemistry. Changing sonic frequency alters the resonant size of the cavitation event and to some extent, the lifetime of the bubble collapse, but the overall process remains unchanged. Sonochemistry is therefore less influenced over the range where cavitation can occur (from tens of Hz to a few MHz). The observed sonochemical rates may change, but well-controlled comparisons of efficiency are lacking at this time and will prove difficult. Subtle differences in product distributions from homogeneous reactions have been occasionally

reported (48). At very high frequencies (above a few MHz), cavitation ceases, and sonochemistry is generally not observed.

Acoustic intensity has a dramatic influence on the observed rates of sonochemical reactions. Below a threshold value, the amplitude of the sound field is too small to induce nucleation or bubble growth. Above the cavitation threshold, increased intensity of irradiation (from an immersion horn, for example) will increase the effective volume of the zone of liquid which will cavitate, and thus, increase the observed sonochemical rate. Furthermore, as the acoustic pressures increase, the range of bubble sizes which will undergo transient cavitation increases; this too will increase the observed sonochemical rate. It is often observed experimentally, however, that as one continues to increase acoustic amplitude, eventually rates begin to diminish. At high intensities, the cavitation of the liquid near the radiating surface becomes so intense as to produce a shroud of bubbles which will diminish the penetration of the sound into the liquid. In addition, bubble growth may become so rapid that the bubble grows beyond the size range of transient cavitation before implosive collapse can occur.

The effect of the bulk solution temperature lies primarily in its influence on the bubble content before collapse. With increasing temperature, in general, sonochemical reaction rates are *slower*! This reflects the dramatic influence which solvent vapor pressure has on the cavitation event: the greater the solvent vapor pressure found within a bubble prior to collapse, the less effective the collapse. There is generally a linear correlation of the log of the sonochemical rate and the total solvent vapor pressure (49). When secondary reactions are being monitored (as in chemical reactions occurring after initial acoustic erosion of a passivated surface), temperature will play its usual role in thermally activated chemical reactions. This explains the common observation that rates of heterogeneous sonochemistry often have an optimal reaction temperature: below this temperature, cavitational processes are improved, but secondary chemical reactions are slowed, and at higher temperatures, vice versa.

Increases in the applied static pressure increase the acoustic intensity necessary for cavitation, but if equal number of cavitation events occur, the collapse should be more intense. In contrast, as the ambient pressure is reduced, eventually the gas-filled crevices of particulate matter which serve as nucleation sites for the formation of cavitation in even "pure" liquids, will be deactivated, and therefore the observed sonochemistry will be diminished.

The choice of ambient gas will also have a major impact on sonochemical reactivity. The maximum temperature reached during cavitation is strongly dependent on the polytropic ratio ($\gamma = C_p/C_v$) of the ambient gas, which defines the amount of heat released during the adiabatic compression of that gas. Monatomic gases give much more heating than diatomic, which are much better than polyatomic gases (including solvent vapor). Sonochemical rates are also significantly influenced by the thermal conductivity of the ambient, so even the noble gases affect cavitation differently: He is generally much worse than Ar and Xe is the best; Ar is often the most cost-effective choice. In addition, sonochemical reactions will often involve the gases present in the cavitation event.

The choice of the solvent also has a profound influence on the observed sonochemistry. The effect of vapor pressure has already been mentioned. Other

liquid properties, such as surface tension and viscosity, will alter the threshold of cavitation, but this is generally a minor concern. The chemical reactivity of the solvent is often much more important. No solvent is inert under the high temperature conditions of cavitation (50). One may minimize this problem, however, by using robust solvents that have low vapor pressures so as to minimize their concentration in the vapor phase of the cavitation event. Alternatively, one may wish to take advantage of such secondary reactions, for example, by using halocarbons for sonochemical halogenations. With ultrasonic irradiations in water, the observed aqueous sonochemistry is dominated by secondary reactions of OH· and H· formed from the sonolysis of water vapor in the cavitation zone (51–53).

Control of sonochemical reactions is subject to the same limitation that any thermal process has: the Boltzmann energy distribution means that the energy per individual molecule will vary widely. One does have easy control, however, over the energetics of cavitation through the parameters of acoustic intensity, temperature, ambient gas, and solvent choice. The thermal conductivity of the ambient gas (eg, a variable He/Ar atmosphere) and the overall solvent vapor pressure provide easy methods for the experimental control of the peak temperatures generated during the cavitational collapse.

Homogeneous Sonochemistry: Bond Breaking and Radical Formation. The chemical effect of ultrasound on aqueous solutions have been studied for many years. The primary products are H_2 and H_2O_2; there is strong evidence for various high-energy intermediates, including HO_2, H·, OH·, and perhaps $e^-_{(aq)}$. The elegant work of Riesz and collaborators used electron paramagnetic resonance with chemical spin-traps to demonstrate definitively the generation of H· and OH· during ultrasonic irradiation, even with clinical sources of ultrasound (51–53). The extensive work in Henglein's laboratory involving aqueous sonochemistry of dissolved gases has established clear analogies to combustion processes (27,28). As one would expect, the sonolysis of water, which produces both strong reductants and oxidants, is capable of causing secondary oxidation and reduction reactions, as often observed by Margulis and co-workers (54). Most recently there has been strong interest shown in the use of ultrasound for remediation of low levels of organic contamination of water (47,55,56). The OH· radicals produced from the sonolysis of water are able to attack essentially all organic compounds (including halocarbons, pesticides, and nitroaromatics) and through a series of reactions oxidize them fully. The desirability of sonolysis for such remediation lies in its low maintenance requirements and the low energy efficiency of alternative methods (eg, ozonolysis, uv photolysis).

In contrast, the ultrasonic irradiation of organic liquids has been less studied. Suslick and co-workers established that virtually all organic liquids will generate free radicals upon ultrasonic irradiation, as long as the total vapor pressure is low enough to allow effective bubble collapse (49). The sonolysis of simple hydrocarbons (for example, *n*-alkanes) creates the same kinds of products associated with very high temperature pyrolysis (50). Most of these products (H_2, CH_4, and the smaller 1-alkenes) derive from a well-understood radical chain mechanism.

The sonochemistry of solutes dissolved in organic liquids also remains largely unexplored. The sonochemistry of metal carbonyl compounds is an

exception (57). Detailed studies of these systems led to important mechanistic understandings of the nature of sonochemistry. A variety of unusual reactivity patterns have been observed during ultrasonic irradiation, including multiple ligand dissociation, novel metal cluster formation, and the initiation of homogeneous catalysis at low ambient temperature (57).

Applications of Sonochemistry to Materials Synthesis. Of special interest is the recent development of sonochemistry as a synthetic tool for the creation of unusual inorganic materials (58,59). As one example, the recent discovery of a simple sonochemical synthesis of amorphous iron (Fig. 10) helped settle the longstanding controversy over its magnetic properties (60,61). More generally, ultrasound has proved extremely useful in the synthesis of a

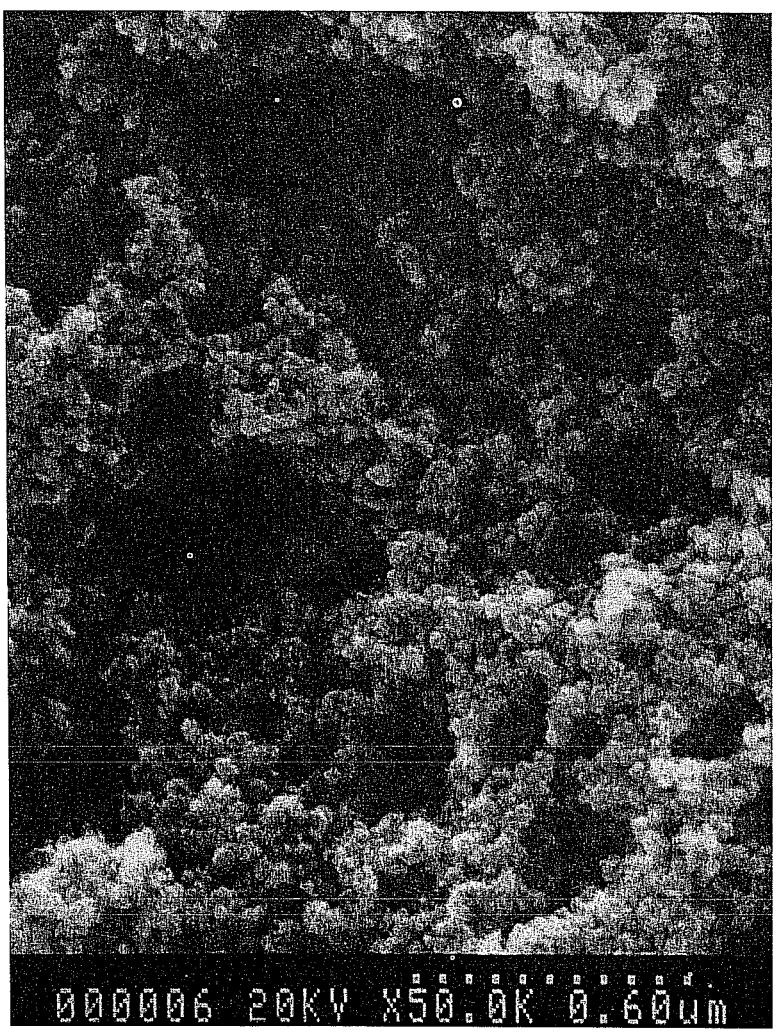

Fig. 10. Scanning electron micrograph of amorphous nanostructured iron powder produced from the ultrasonic irradiation of $Fe(CO)_5$. Reproduced with permission (60).

wide range of nanostructured materials, including high surface area transition metals, alloys, carbides, oxides and colloids (62,64). Sonochemical decomposition of volatile organometallic precursors in high boiling solvents produces nanostructured materials in various forms with high catalytic activities. Nanometer colloids, nanoporous high surface area aggregates, and nanostructured oxide supported catalysts can all be prepared by this general route, as shown schematically in Figure 11. For example, sonication of iron pentacarbonyl with silica generated an amorphous nanostructured $Fe–SiO_2$ supported catalyst. This catalyst showed higher catalytic activity for the Fischer-Tropsch synthesis compared to the conventional Fe–silica catalyst prepared by the traditional incipient wetness method. Sonochemical synthesis of high surface area alloys can be accomplished by the sonolysis of $Fe(CO)_5$ and $Co(CO)_3(NO)$. As another example, ultrasonic irradiation of $Mo(CO)_6$ produces aggregates of nanometer-sized clusters of face centered cubic molybdenum carbide. The extremely porous material had a high surface area and consisted of aggregates of ≈2-nm sized particles. The catalytic properties showed that the molybdenum carbide generated by ultrasound is an active and highly selective dehydrogenation catalyst comparable to commercial ultrafine platinum powder.

Sonochemistry is also proving to have important applications with polymeric materials. Substantial work has been accomplished in the sonochemical initiation of polymerization and in the modification of polymers after synthesis (3,5). The use of sonolysis to create radicals which function as radical initiators has been well explored. Similarly the use of sonochemically prepared radicals and other reactive species to modify the surface properties of polymers is being developed, particularly by G. Price. Other effects of ultrasound on long chain polymers tend to be mechanical cleavage, which produces relatively uniform size distributions of shorter chain lengths.

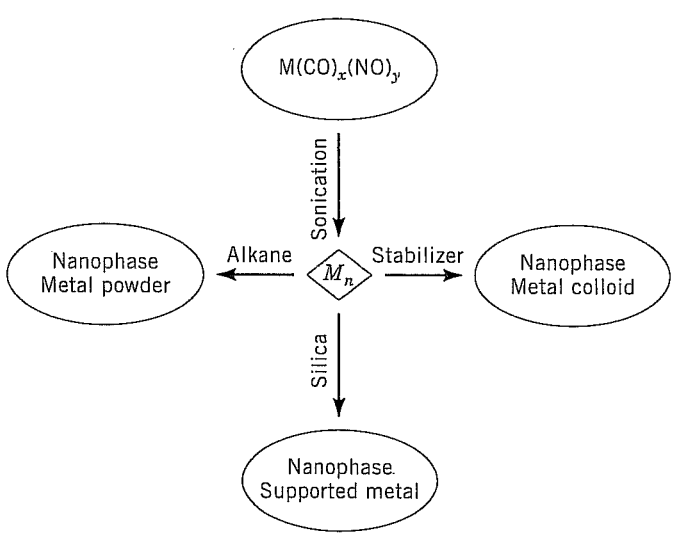

Fig. 11. Sonochemical synthesis of various forms of nanostructured materials. n = 100–1000.

Another important application has been the sonochemical preparation of biomaterials, most notably protein microspheres (65–68). Using high intensity ultrasound and simple protein solutions, a remarkably easy method to make both air-filled microbubbles and nonaqueous liquid-filled microcapsules has been developed. Figure 12 shows an electron micrograph of sonochemically prepared microspheres. These microspheres are stable for months, and being slightly smaller than erythrocytes, can be intravenously injected to pass unimpeded through the circulatory system. The mechanism responsible for microsphere formation is a combination of *two* acoustic phenomena: emulsification and cavitation. Ultrasonic emulsification creates the microscopic dispersion of the protein solution necessary to form the proteinaceous microspheres. Alone, however, emulsification is insufficient to produce long-lived microspheres. The long life of these microspheres comes from a sonochemical cross-linking of the protein shell. Protein cysteine residues are oxidized during microsphere formation by sonochemically produced superoxide. These protein microspheres, have a wide range of biomedical applications, including their use as echo contrast agents for sonography, magnetic-resonance-imaging contrast enhancement, drug delivery, among others.

Heterogeneous Sonochemistry: Reactions of Solids with Liquids. The use of ultrasound to accelerate chemical reactions in heterogeneous systems has

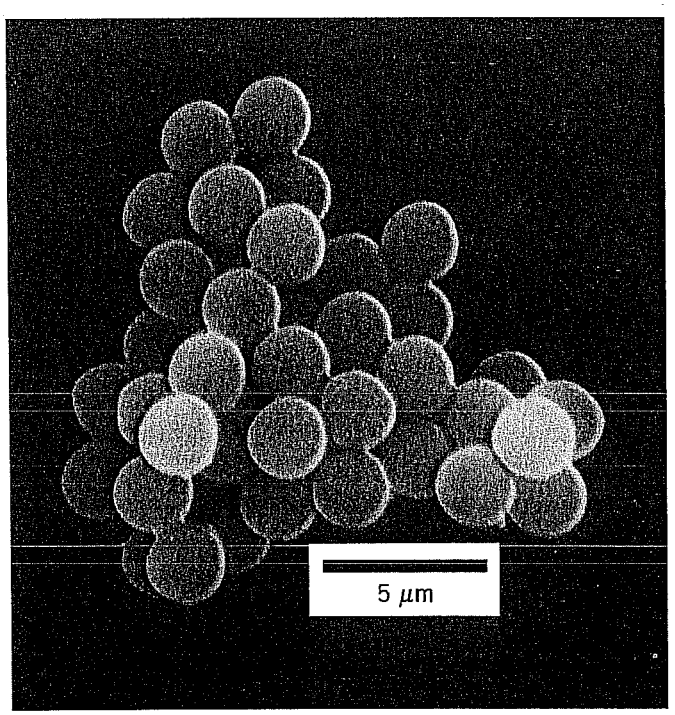

Fig. 12. Scanning electron micrograph of sonochemically synthesized hemoglobin microspheres.

become increasingly widespread. The physical phenomena which are responsible include the creation of emulsions at liquid–liquid interfaces, the generation of cavitational erosion and cleaning at liquid–solid interfaces, the production of shock wave damage and deformation of solid surfaces, the enhancement in surface area from fragmentation of friable solids, and the improvement of mass transport from turbulent mixing and acoustic streaming.

The use of high-intensity ultrasound to enhance the reactivity of reactive metals as stoichiometric reagents has become an especially routine synthetic technique for many heterogeneous organic and organometallic reactions (11–15), particularly those involving reactive metals, such as Mg, Li or Zn. This development originated from the early work of Renaud and the more recent breakthroughs of Luche (12,13). The effects are quite general and apply to reactive inorganic salts and to main group reagents as well (69). Less work has been done with unreactive metals (eg, V, Nb, Mo, W), but results here are promising as well (11). Rate enhancements of more than tenfold are common, yields are often substantially improved, and by-products avoided. A wide range of synthetically useful heterogeneous sonochemical reactions have been listed in Table 1. The applications of sonochemistry to organic synthesis have been reviewed recently in great detail (13).

The mechanism of the sonochemical rate enhancements in both stoichiometric and catalytic reactions of metals is associated with dramatic changes in morphology of both large extended surfaces and of powders. As discussed earlier, these changes originate from microjet impact on large surfaces and high-velocity interparticle collisions in slurries. Surface composition studies by Auger electron spectroscopy and sputtered neutral mass spectrometry reveal that ultrasonic irradiation effectively removes surface oxide and other contaminating coatings (11). The removal of such passivating coatings can dramatically improve reaction rates. The reactivity of clean metal surfaces also appears to be responsible for the greater tendency for heterogeneous sonochemical reactions to involve single electron transfer rather than acid–base chemistry (70).

Applications of ultrasound to electrochemistry have also seen substantial recent progress. Beneficial effects of ultrasound on electroplating and on organic synthetic applications of organic electrochemistry (71) have been known for quite some time. More recent studies have focused on the underlying physical theory of enhanced mass transport near electrode surfaces (72,73). Another important application for sonoelectrochemistry has been developed by J. Reisse and co-workers for the electroreductive synthesis of sub-micrometer powders of transition metals (74).

Sonocatalysis. Ultrasound has potentially important applications in both homogeneous and heterogeneous catalytic systems. The inherent advantages of sonocatalysis include (*1*) the use of low ambient temperatures to preserve thermally sensitive substrates and to enhance selectivity; (*2*) the ability to generate high energy species difficult to obtain from photolysis or simple pyrolysis; and (*3*) the mimicry of high temperature and pressure conditions on a microscopic scale.

Homogeneous catalysis of various reactions often uses organometallic compounds. The starting organometallic compound, however, is often catalytically inactive until loss of metal-bonded ligands (such as carbon monoxide) from the

Table 1. Some Representative Examples of Heterogeneous Sonochemistry

Heterogeneous reagent	Reactant	Products
Compounds of metals		
$LiAlH_4$	Ar-X	ArH
$LiAlH_4$	R_3M-X (X = Cl, NR_2, OR)	R_3M-H (M = Si, Ge, Sn)
Al_2O_3	$C_6H_5CH_2Br$ + KCN	$C_6H_5CH_2CN$
$KMnO_4$	RR′HCOH	RR′CO
CrO_2Cl_2	RR′HCOH	RR′CO
HBR_2	$R'_2C{=}CR'_2$	HR'_2C-$CR'_2(BR_2)$
MS_2, M = Mo, Ta, Zr	NR_3, py, Cp_2Co	intercalates
Hg	$(HR_2BrC)_2CO$ + R′CO_2H	$(HR_2C)CO(C(O_2CR')R_2)$
	$(HR_2BrC)_2CO$ + R′OH	$(HR_2C)CO(C(OR')R_2)$
Mg	R-Br	R-MgBr
	$R_2C{=}CHCH_2Cl$ + $Mg/C_{14}H_{14}$	$R_2C{=}CHCH_2MgCl$
Li	R-Br (R = C_3H_6, *m*-C_4H_9, C_6H_5)	R-Li
	R-Br + R′R″CO	RR′R″COH
	R-Br + $(H_3C)_2NCHO$	RCHO
	R_3M-Cl (M = C, Si, Sn)	R_3MMR_3
	R_2SiCl_2 (R = arenes)	cyclo-$(R_2Si)_3$
	R_2MCl_2 + Na + Se (M = Si, Sn)	$(R_2MSe)_3$

Zn	$CF_3I + RR'C{=}O$	$RR'C(OH)CF_3$
	$C_nF_{2n+1}I + CO_2$	$C_nF_{2n+1}CO_2H$
	$RR'C{=}O + BrCH_2CO_2R''$	$RR'C(OH)CH_2CO_2R''$
	$C_6H_5Br + RCOCH{=}CHR' + Ni(acac)_2$	$RCOCH_2CHR'C_6H_5$ (R = H, alkyl)
	$RR'C{=}O + R''_2C{=}CHCH_2Br$	$RR'(HO)CCR''_2CH{=}CH_2$
Transition metals	$MCl_5 + Na + CO$ (M = V, Nb, Ta)	$M(CO)_6^-$
	$MCl_6 + Na + CO$ (M = Cr, Mo, W)	$M_2(CO)_{10}^{-2}$
	$MnCl_3 + Na + CO$	$Mn(CO)_5^-$
	$FeCl_3 + Na + CO$	$Fe(CO)_4^{-2} + Fe_2(CO)_8^{-2}$
	$Fe_2(CO)_9$ + alkenylepoxide	$Fe(CO)_3$(π-allyllactone)
	$Fe_2(CO)_9 + RHC{=}CR'\text{-}CH{=}CHR'$	$Fe(CO)_3$(η^4-diene)
	$NiCl_2 + Na + CO$	$Ni_6(CO)_{12}^{-2}$
	$NiCl_2 + Na$ + bipy + COD/CDT	Ni(bipy)(COD/CDT)
	$Co(acac)_3 + C_5H_6$ + COD + $Mg/C_{14}H_{10}$	Co(Cp)(COD)
	$RuCl_3$ + Li + 1,5-cyclooctadiene	(η^6-1,3,5-COT)(η^4-1,5-COD)Ru(0)
	$[Fe(C_5R_5)(CO)_2]_2 + K + (C_6H_5)_3C^+$	$Fe(C_5R_5)(CO)_2(C_2H_4)^+$
	$[M(C_5R_5)(CO)_n]_2 + K$ (M = Fe, Ru, Mo)	$[M(C_5R_5)(CO)_n]^-$
	$Pd + CH_2{=}CHCH_2X$	$[(\eta^3\text{-}H_2C\text{–}CH\text{–}CH_2)Pd(X)]_2$
	La + NH_4SCN in HMPA	$La(NCS)_3 \cdot 4HMPA$
	Cu + o-$C_6H_4(NO_2)I$	o-$(O_2N)H_4C_6\text{–}C_6H_4(NO_2)$

metal. Having demonstrated that ultrasound can induce ligand dissociation, the initiation of homogeneous catalysis by ultrasound becomes practical. A variety of metal carbonyls upon sonication will catalyze the isomerization of 1-alkenes to the internal alkenes (57), through reversible hydrogen atom abstraction, with rate enhancements of as much as 10^5 over thermal controls.

Heterogeneous catalysis is generally more industrially important than homogeneous systems, and the applications of ultrasound here have been reviewed recently (75). Heterogeneous catalysts often require rare and expensive metals. The use of ultrasound offers some hope of activating less reactive, but also less costly, metals. Such effects can occur in three distinct stages: (*1*) during the formation of supported catalysts, (2) activation of pre-formed catalysts, or (*3*) enhancement of catalytic behavior during a catalytic reaction. Some early investigations of the effects of ultrasound on heterogeneous catalysis can be found in the Soviet literature (76). In this early work, increases in turnover rates were usually observed upon ultrasonic irradiation, but were rarely more than tenfold. In the cases of modest rate increases, it appears likely that the cause is increased effective surface area; this is especially important in the case of catalysts supported on brittle solids (77). More impressive accelerations, however, have include hydrogenations and hydrosilations by Ni powder, Raney Ni, and Pd or Pt on carbon. For example, as shown in Figure 13, the hydrogenation of alkenes

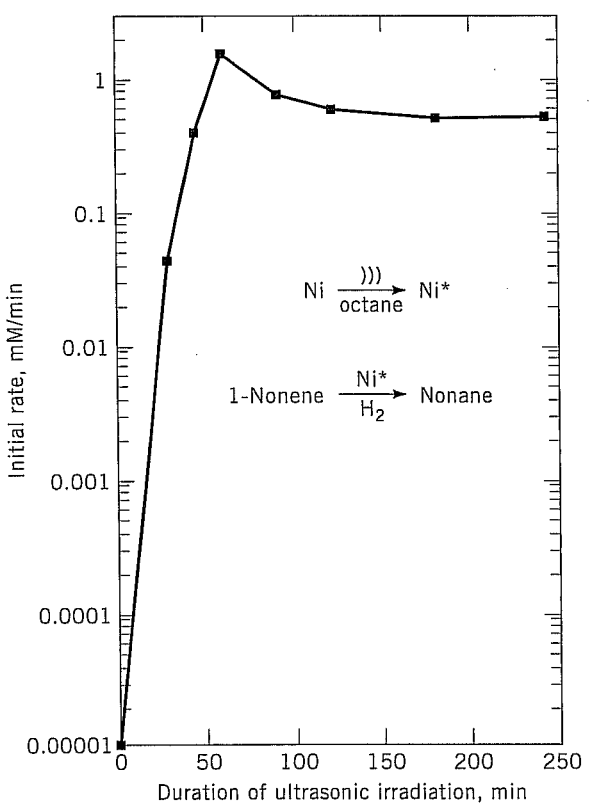

Fig. 13. The effect of ultrasonic irradiation on the catalytic hydrogenation activity of Ni powder. Reproduced with permission (16).

by Ni powder is enormously enhanced (>10^5-fold) by ultrasonic irradiation (16). This dramatic increase in catalytic activity is due to the formation of uncontaminated metal surfaces from interparticle collisions caused by cavitation-induced shockwaves.

Summary

The phenomenon of acoustic cavitation results in an enormous concentration of energy. If one considers the energy density in an acoustic field that produces cavitation and that in the collapsed cavitation bubble, there is an amplification factor of over eleven orders of magnitude. The enormous local temperatures and pressures so created result in phenomena such as sonochemistry and sonoluminescence and provide a unique means for fundamental studies of chemistry and physics under extreme conditions. A diverse set of applications of ultrasound to enhancing chemical reactivity has been explored, with important applications in mixed-phase synthesis, materials chemistry, and biomedical uses.

BIBLIOGRAPHY

1. K. S. Suslick, ed., *Ultrasound: Its Chemical, Physical, and Biological Effects*, VCH Publishers, New York, 1988.
2. K. S. Suslick, *Science* **247**, 1439 (1990).
3. T. J. Mason, ed., *Advances in Sonochemistry*, vols. 1–4, JAI Press, New York, 1990, 1991, 1993, 1996.
4. T. J. Mason and J. P. Lorimer, *Sonochemistry: Theory, Applications and Uses of Ultrasound in Chemistry*, Ellis Horword, Ltd., Chichester, U.K., 1988.
5. G. J. Price, ed., *Current Trends in Sonochemistry*, Royal Society of Chemistry, Cambridge, 1992.
6. K. S. Suslick, D. A. Hammerton, and R. E. Cline, Jr., *J. Am. Chem. Soc.* **108**, 5641 (1986).
7. E. B. Flint and K. S. Suslick, *Science* **253**, 1397 (1991).
8. L. A. Crum, *Proc. 1982 Ultrasonics Symp.* **1**, 1 (1982).
9. T. G. Leighton, *The Acoustic Bubble*, Academic Press, London, 1994, pp. 531–551.
10. S. J. Doktyez and K. S. Suslick, *Science* **247**, 1067 (1990).
11. K. S. Suslick and S. J. Doktycz, *Adv. Sonochem.* **1**, 197–230 (1990).
12. C. Einhorn, J. Einhorn, and J.-L. Luche, *Synthesis*, 787 (1989).
13. J. L. Luche, *Comptes Rendus Serie IIB* **323**, 203, 337 (1996).
14. J. M. Pestman, J. B. F. N. Engberts, and F. de Jong, *Recl. Trav. Chim. Pays-Bas* **113**, 533 (1994).
15. K. S. Suslick, "Sonochemistry of Transition Metal Compounds," in R. B. King, ed., *Encyclopedia of Inorganic Chemistry*, John Wiley & Sons, Inc., New York, vol. 7, pp. 3890–3905.
16. K. S. Suslick and D. J. Casadonte, *J. Am. Chem. Soc.* **109**, 3459 (1987).
17. L. A. Crum, *Physics Today* **47**, 22 (1994).
18. S. J. Putterman, *Scientific American*, 46 (Feb. 1995).
19. Lord Rayleigh, *Philos. Mag.* **34**, 94 (1917).
20. W. T. Richards and A. L. Loomis, *J. Am. Chem. Soc.* **49**, 3086 (1927).
21. M. A. Margulis, *Ultrasonics* **30**, 152 (1992).
22. T. Lepoint and F. Mullie, *Ultrasonics Sonochem.* **1**, S13 (1994).

23. H. G. Flynn, "Physics of Acoustic Cavitation in Liquids," in W. P. Mason, ed., *Physical Acoustics*, vol. 1B, Academic Press, New York, 1964, p. 157.
24. L. A. Crum, *J. Acoust. Soc. Am.* **95**, 559 (1994).
25. B. P. Barber and S. J. Putterman, *Phys. Rev. Lett.* **69**, 3839 (1992).
26. R. Lofstedt, B. P. Barber, and S. J. Putterman, *Phys. Fluids A* **5**, 2911 (1993).
27. A. Henglein, *Ultrasonics* **25**, 6 (1985).
28. A. Henglein, *Adv. Sonochem.* **3**, 17 (1993).
29. H. Frenzel and H. Schultes, *Z. Phys. Chem.* **27b**, 421 (1934).
30. T. J. Matula, R. A. Roy, P. D. Mourad, W. B. McNamara III, and K. S. Suslick, *Phys. Rev. Lett.* **75**, 2602 (1995).
31. D. F. Gaitan and L. A. Crum, in D. T. Blackstock, ed., *Frontiers of Nonlinear Acoustics*, 12th ISNA, Elsevier Applied Science, New York, 1990, pp. 459–463.
32. D. F. Gaitan, L. A. Crum, R. A. Roy, and C. C. Church, *J. Acoust. Soc. Am.* **91**, 3166 (1992).
33. B. P. Barber, R. A. Hiller, R. Lofstedt, S. J. Putterman, and K. R. Weninger, *Phys. Rev. Lett.* **72**, 1380 (1994).
34. L. A. Crum and R. A. Roy, *Science* **266**, 233 (1994).
35. R. E. Verrall and C. Sehgal in Ref. 1, pp. 227–287.
36. E. B. Flint and K. S. Suslick, *J. Phys. Chem.* **95**, 1484 (1991).
37. E. B. Flint and K. S. Suslick, *J. Amer. Chem. Soc.* **111**, 6987 (1989).
38. R. Hiller, K. Weninger, S. J. Putterman, and B. P. Barber, *Science* **266**, 248 (1994).
39. B. P. Barber, R. Hiller, K. Arisaka, H. Fetterman, and S. J. Putterman, *J. Acoust. Soc. Am.* **91**, 3061 (1992).
40. B. P. Barber, C. C. Wu, R. Lofstedt, P. H. Roberts, and S. J. Putterman, *Phys. Rev. Lett.* **72**, 1380 (1994).
41. W. C. Moss, D. B. Clarke, and D. A. Young, *Science* **276**, 1398 (1997).
42. D. Lohse and co-workers, *Phys. Rev. Lett.* **78**, 1359 (1997).
43. J. Berlan and T. J. Mason, *Ultrasonics* **30**, 203 (1992).
44. T. J. Mason and E. D. Cordemans, *Chem. Eng. Res. Des.* **74**, 511 (1996).
45. R. L. Hunicke, *Ultrasonics* **28**, 291 (1990).
46. A. Shoh in Ref. 1, pp. 97–122.
47. J. Reisse, T. Caulier, C. Deckerkheer, O. Fabre, J. Vandercammen, J. L. Delplancke, and R. Winand, *Ultrason. Sonochem.* **3**, S147 (1996).
48. C. Petrier and S. Laguian, *Chemosphere* **32**, 1709 (1996).
49. K. S. Suslick, J. W. Gawienowski, P. F. Schubert, and H. H. Wang, *Ultrasonics* **22**, 33 (1984).
50. K. S. Suslick, J. W. Gawienowski, P. F. Schubert, and H. H. Wang, *J. Phys. Chem.* **87**, 2229 (1983).
51. P. Riez, *Adv. Sonochem.* **2**, 23 (1991).
52. V. Misik and P. Riesz, *Ultrason. Sonochem.* **3**, S173 (1996).
53. P. Riesz, D. Berdahl, and C. L. Christman, *Environ. Health Perspect.* **64**, 233 (1985).
54. M. A. Margulis and N. A. Maximenko, *Adv. Sonochem.* **2**, 253 (1991).
55. M. R. Hoffmann, I. Hua, and R. Hochemer, *Ultrasonics Sonochemistry* **3**, S163 (1996).
56. I. Hua, R. H. Hochemer, and M. R. Hoffmann, *Env. Sci. Tech.* **29**, 2790 (1995).
57. K. S. Suslick, *Adv. Organomet. Chem.* **25**, 73 (1986).
58. K. S. Suslick, *MRS Bull.* **20**, 29 (1995).
59. O. V. Abramov, *Ultrasound in Liquid and Solid Metals*, CRC Press, Boca Raton, Fla., 1994.
60. K. S. Suslick, S. B. Choe, A. A. Cichowlas, and M. W. Grinstaff, *Nature* **353**, 414 (1991).
61. M. W. Grinstaff, M. B. Salamon, and K. S. Suslick, *Phys. Rev. B* **48**, 269 (1993).
62. K. S. Suslick, T. Hyeon, and M. Fang, *Chem. Mater.* **8**, 2172 (1996).

63. T. Hyeon, M. Fang, and K. S. Suslick, *J. Am. Chem. Soc.* **118**, 5492 (1996).
64. K. S. Suslick, M. Fang, and T. Hyeon, *J. Am. Chem. Soc.* **118**, 11960 (1996).
65. K. S. Suslick and M. W. Grinstaff, *J. Am. Chem. Soc.* **112**, 7807 (1990).
66. K. S. Suslick and M. W. Grinstaff, *Proc. Natl. Acad. Sci. USA* **88**, 7708 (1991).
67. K. J. Liu, M. W. Grinstaff, J. Jiang, K. S. Suslick, H. M. Swartz, and W. Wang, *Biophys. J.* **67**, 896 (1994).
68. A. G. Webb, M. Wong, K. J. Kolbeck, R. L. Magin, L. J. Wilmes, and K. S. Suslick, *J. Mag. Res. Imaging* **6**, 675 (1996).
69. T. Ando and T. Kimura, *Adv. Sonochem.* **2**, 211 (1991).
70. J.-L. Luche, *Ultrasonics Sonochem.* **1**, S111 (1994).
71. A. Durant, H. Francois, J. Reisse, and A. Kirschdemesmaeker, *Electrochim. Acta* **41**, 277 (1996).
72. R. G. Compton, J. C. Eklund, and F. Marken, *Electroanalysis.* **9**, 509 (1997).
73. N. A. Madigan and L. A. Coury, *Anal. Chem.* **69**, 5 (1997).
74. A. Durant, J. L. Delplancke, R. Winand, and J. Reisse, *Tetrahedron Lett.* **36**, 4257 (1995).
75. K. S. Suslick, "Sonocatalysis," in G. Ertl, H. Knozinger, and J. Weitkamp, eds., *Handbook of Heterogeneous Catalysis*, vol. 3, Wiley-VCH, Weinheim, 1997, Chapt. 8.6, pp. 1350–1357.
76. A. N. Mal'tsev, *Zh. Fiz. Khim.* **50**, 1641 (1976).
77. B. H. Han and P. Boudjouk, *Organometallics* **2**, 769 (1983).

KENNETH S. SUSLICK
University of Illinois at Urbana-Champaign